Green Chemistry

Accepted Manuscript

ROYAL SOCIETY OF CHEMISTRY

www.rsc.org/greenchem

Cite this: DOI: 10.1039/c0xx00000x

www.rsc.org/xxxxxx

ARTICLE TYPE

Perovskite Type Oxide Supported Ni Catalysts for the Production of 2,5-Dimethylfuran from Biomass-Derived 5-Hydroxymethylfurfural†

Meng-Yuan Chen,[a] **‡ Chu-Bai Chen,**[a]**‡ Bakht Zada,**[a] **and Yao Fu**[a]*****

Received (in XXX, XXX) Xth XXXXXXXXX 20XX, Accepted Xth XXXXXXXXX 20XX
DOI: 10.1039/b000000x

The hydrogenolysis of C-O and C=O in 5-hydroxymethylfurfural for the production of furan biofuel 2,5-dimethylfuran is of great importance for biomass refining. However, development of non-noble metal based catalysts which perform stably for this process is still challenging. Here, perovskite supported Ni catalysts were used for the hydrogenolysis of 5-hydroxymethylfurfural at 230 °C, and 98.3% yield of DMF was obtained. The effect of reaction conditions such as temperature and pressure were investigated and discussed, and the catalyst could maintain good activity after used for at least 5 times. In order to further explore the reaction mechanism, dynamic experiments at different time were carried out and a possible reaction pathway was proposed. The development of efficient perovskite supported Ni catalysts verified the great potential in biomass conversion.

1 Introduction

With the gradual decrease of the fossil resources which is not sustainable, the demand for exploring the renewable feedstock for the production of transportation fuel and chemicals is getting more and more attention.[1] Biomass, which is widespread, abundant all over the world, inexpensive, and renewable, is considered to be an ideal promising alternative to fossil resources for the production of fuels and chemicals.[2] However, because of the high oxygen-content in biomass-derived compounds (*e.g.* 5-hydroxymethylfurfural (HMF), levulinic acid (LA), furfural, phenol and guaiacol, etc.), they could not be directly used as renewable fuels.[3] Hydrogenolysis is an important process for the deoxygenation of these oxygen-containing compounds.[4] A representative and important process is the hydrogenolysis of HMF to afford the bio-fuel 2,5-dimethylfuran (DMF).[5] In this case, HMF is an important bio-based compound which is affirmed as one of the top 10 platform molecules derived from biomass.[6] It can be converted into 2,5-furandimethanol (FDM)[7] and furan 2,5-dicarboxylic acid (FDCA)[8] through hydrogenation and oxidation, respectively, which could be used for the polymer industry. DMF could be obtained through further hydrogenolysis of HMF, which is considered as a highly promising new generation of alternative liquid fuel.[9]

Compare to bio-ethanol and bio-butanol, which are studied deeply as alternative energy sources,[10] DMF shows a lot of advantages. According to the previous report on the physicochemical properties of DMF, bio-ethanol and bio-butanol,[11] DMF has higher lower heating value (LHV, 33.7 MJ/kg, 26.9 MJ/kg, 33.2 MJ/kg for DMF, bio-ethanol and bio-butanol, respectively) which will cost less fuel. The boiling point of DMF (93 °C)[12a] is higher than that of bio-ethanol (77.3 °C) and lower than that of bio-butanol (117.25 °C), which is in favor of suppressing the vapor lock in the inlet and the cold starting performance at low ambient temperature respectively. The water solubility of DMF at 20 °C is just 0.26wt%, however bio-ethanol is miscible with water, the water solubility of bio-butanol is 7.7wt% at 20 °C, this advantage makes DMF harder to absorb water from air which will reduce the product quality. The kinematic viscosity of DMF at 20 °C (0.57 cSt) is similar to that of gasoline (0.37-0.44 cSt), which is advantageous to establishing the injection pressure of DMF in fuel system and protecting the movements in the engine components, for comparison, the kinematic viscosity of bio-ethanol and bio-butanol at 20 °C are 1.5 cSt and 3.6 cSt, respectively. Moreover, the research octane number (RON)[12,5] of DMF (119) is higher than that of bio-ethanol, bio-butanol and gasoline (110, 98, 90-100 respectively). These advantages mentioned above makes DMF a promising bio-fuel.

Dumesic et al. firstly published the reaction pathway for the production of DMF from fructose, CuRu/C[5] was used for the hydrogenolysis of HMF with a yield of 76-79%. In general, the subsequent reports on the selective hydrogenolysis of HMF were mainly performed over noble metals (*e.g.* Pd/C[13], Ru/C[14], RuSn/C[15], Ru-K-OMS-2[16], Pd_xAu_y/C[17], Pd/C/Zn[18], Pd/Fe_2O_3[19], PtCo@HCS[20], Ru/Co_3O_4[21], $Ru/Cu/Fe_3O_4$/N-rGO[22], Pt/C[23], Ru/HT[24], Ru-Sn/ZnO[25], Ru-NaY[12c]). Development of non-precious metal based catalysts for this hydrogenolysis process is of great importance for the industrial application of DMF. However, because of the generally low activity of non-noble metal catalysts[26], only few studies reported the construction of non-noble metal catalysts for the hydrogenolysis of HMF. Currently, the reported non-noble metal catalyst systems for the conversion of HMF into DMF can be divided into two categories: (1) nickel based catalysts, *e. g.* Raney Ni[27], $Ni\text{-}Al_2O_3$ derived from hydrotalcite-like compounds[28], nickel nanoparticles inlaid nickel phyllosilicata (NiSi-PS)[29], Ni/Co_3O_4[30], Ni-Fe/CNT[31]; (2) copper based catalysts, *e. g.* Cu-doped porous metal oxide (Cu-PMO)[32], copper-zine nanoalloy nanopowder (CuZn)[33], Cu-ZnO catalysts derived from minerals (*e.g.* malachite)[34]. Recent progress on the properties and production of DMF were also reviewed in some reports[7h,11,12a,35]. Nickel based catalysts are more attractive because they are active for the cracking of the C-O bonds in the biomass derived molecular under relatively mild conditions[29]. Recently, our group proposed the non-noble bimetallic $Ni-W_2C/AC$ catalyst for the hydrogenolysis of HMF and gave rise to a 96% yield of DMF[36]. Nevertheless, the establishment of novel non-noble catalyst systems which can be synthesized simply and perform steadily is particularly essential for the industrial production of bio-fuel DMF.

Perovskite-type functional materials are widely studied in the fields of catalysis[37], fuel cell[38] and solar cell[39], especially catalytic hydrogenation[40]. And the high thermal and hydrothermal stability of perovskite oxides enable them appropriate for catalysis[37c]. Recently perovskite-type oxide catalysts which can be represented by the general formula ABO_3[41] structures were gradually found to be efficient for bio-refinery process, for instance, steam reforming of ethanol[42], hydrogenation[43] etc. And it was reported[43] that perovskite-type oxides could help to stabilize the metal particles on the metallic oxides which will effectively improve the activity and stability of the catalysts. In consideration of the advantage of perovskite-based catalysts, non-noble metal nickel supported on perovskte-type oxide supports was synthesized for the investigation of the hydrogenolysis process of biomass-derived HMF. The catalyst showed high activity and selectivity towards DMF, and the catalyst could maintain good activity after used for at least 5 times. The effect of different reaction conditions on the reaction was investigated and a possible reaction mechanism was proposed. The establishment of perovskite-based catalysts highlights its great potential capability for biomass conversion.

2 Experimental

2.1 Materials

HMF, DMF, 2,5-furandimethanol (FDM), 5-methylfurfuryl alcohol (MFA), 2,5-dihydroxymethyltetrahydrofuran (DHMTHF), and 5-methylfurfural (MF) were generously gifted by Hefei Leaf Energy Biotechnology Co., Ltd (www.leafresource.com). Nickel nitrate hexahydrate (99.9+%) was supplied by Strem Chemical, Inc. Iron nitrate nonahydrate (AR), citrate acid monohydrate (AR), polyethylene glycol 400 (CP) and ethanol (AR) were purchased from Sinopharm Chemical Reagent Co., Ltd. Lanthanum nitrate hexahydrate (99.99%) was supplied by Energy Chemical. Tetradecane (99%) was obtained from Aladdin Reagent Co., Ltd.

2.2 Catalyst characterization

The nitrogen adsorption/desorption of the catalysts was measured on a Micromeritics ASAP 2020 analyzer. The specific surface areas of the catalysts were determined through the Barrett-Emmet-Tall (BET) method. An X'pert (PANalytical) diffractometer was used to measure the X-ray power diffraction (XRD) patterns of the catalysts at 40 kV and 40 mA. Transmission electron microscopy (TEM) was performed on a JEOL-2010 electron microscope. The samples were deposited on a Cu grids after ultrasonic dispersion of the samples in ethanol. X-ray photoelectron spectroscopy (XPS) analyses of the prepared catalysts were performed on a Thermo Scientific Escalab 250-X-ray photoelectron spectrometer.

2.3 Catalysts preparation

The perovskite supported Ni catalysts were prepared by one-step citric-complexing method[44]. For a typical catalyst preparation, a precalculated amount of nickel nitrate (10.345 mmol), 10 mmol of iron nitrate, 10 mmol of lanthanum nitrate were well dissolved in deionized water in a 100 ml round bottom flask. A certain amount of citrate acid (36.414 mmol) and polyethylene glycol 400 (7.283 mmol) which were 120 mol% and 24 mol% molar amount of all the metal cations respectively were added to the solution under magnetic stirring. Subsequently the mixture were continued to stir vigorously for another 12 h. Then the mixture was taken into an oil batch and kept at 80 ^oC until spongy solids were formed. The spongy solids were transferred into an oven and dried at 120 ^oC for 24 h. Then the mixture was taken into a furnace and the temperature was raised from room temperature (RT) to 750 ^oC at the rate of 10 $^oC/min$ and kept at 750 ^oC for another 5 h to afford the catalyst precursor. The precursor was reduced in a tube furnace under a N_2/H_2 mixed gas, the flow rates were 100 ml/min and 20 ml/min respectively. The temperature of the tube furnace was raised from RT to 500 ^oC at the rate of 10 $^oC/min$ and kept at 500 ^oC for 4 h. After cooling to RT, the resulted powder was collected. The catalyst prepared by this method was marked as LF-N20, in which the "20" represents the weight percent of Ni in the catalyst. And the preparation procedures for the other catalysts in this work were similar to that of LF-N20.

2.4 Catalyst test

The hydrogenolysis reaction of HMF was carried out in a 25 ml Parr reactor equipped with a magnetic stirrer. In a typical experiment, 1.0 mmol of HMF, 1.0 mmol of n-tetradecane (used as internal standard), 100 mg of the catalyst, and 12 ml of ethanol were added to reactor. Then the reactor was purged with hydrogen for 5 times, and maintained at a specified hydrogen pressure (*e.g.* 5.0 MPa) at ambient temperature. The reaction temperature was kept at a certain value, for instance, 230 ^oC. After the reaction, when the reactor was cooled to RT, the mixture of the products was collected and analyzed by gas chromatograph-mass spectrometer (GC-MS) and gas chromatograph (GC).

3 Results and discussion

3.1 Characterization of the catalysts

The X-ray powder diffraction (XRD) patterns of perovskite type oxides (PTO) supported Ni catalysts were displayed in Fig. 1. The characteristic peaks corresponding to the perovskite type reflections of $LaFeO_3$ (labeled as LF) could be obviously discovered in the XRD patterns of different supported Ni catalysts (labeled as LF-N5, LF-N10, LF-N15, LF-N20, LF-N25, LF-N30, respectively). And the reflection peaks corresponding to metallic Ni phase were found in all the supported Ni catalysts, the intensity of metallic Ni phase reflection signals enhanced with the Ni contents in catalysts. The XRD results of the catalysts were similar to the previous reports[44c]. The dimensions of the metallic Ni phase (D_{MP}) were caculated using the Scherrer formula (Table 1). The XRD results of the iron oxides supported Ni catalyst and lanthanum oxides supported Ni catalyst prepared using the same method were presented in the supporting information and the reflection peaks of the metallic Ni phase could be discovered obviously.

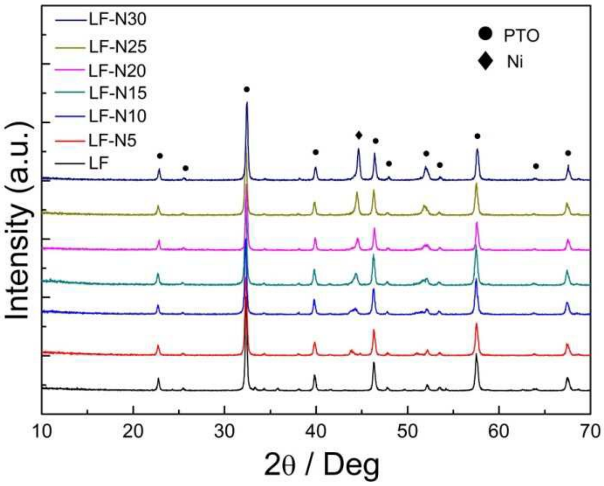

Fig. 1 XRD patterns of perovskite supported Ni catalysts

The TEM images of perovsktite supported catalysts with different Ni contents were also investigated. It could be determined from the TEM images (Fig. 2) that the proper morphologies of the perovskites were prepared in accordance with the previous reports. However, the Ni particles could hardly be observed because it was relatively hard to distinguish the supports and the metallic phase from these TEM images. The TEM images of the iron oxides supported Ni catalyst, lanthanum oxides supported Ni catalyst and $LaFeO_3$ were presented in the supporting information.

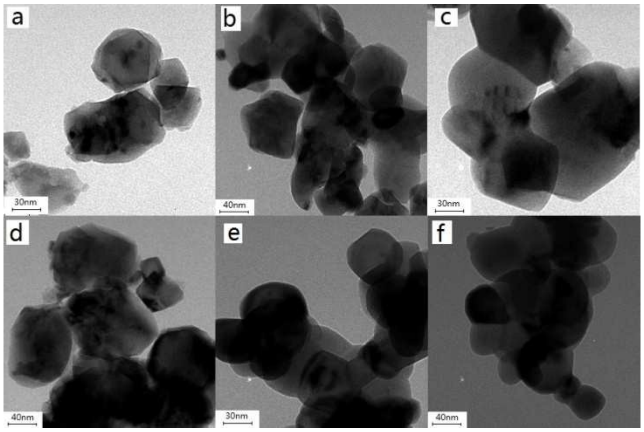

Fig. 2 The TEM images of perovskite supported Ni catalysts with different Ni contents (a) LF-N5; (b) LF-N10; (c) LF-N15; (d) LF-N20; (e) LF-N25; (f) LF-N30

The X-ray photoelectron spectroscopy (XPS) analysis of the supported Ni catalysts was displayed in Fig. 3. Considering that the binding energy (BE) position of La 3d overlapped the BE position of Ni 2p[45], it was hard to measure the BE of Ni 2p, therefore the XPS signals of Ni 3p was analysed. It has been reported that the BE of Ni 3p for metallic Ni is 67 eV[45]. According to the XPS results of the supported Ni catalysts in Fig. 3, the BE of metallic Ni 3p were detected in all the perovskite supported Ni catalysts, indicating the formation of active metallic Ni for the hydrogenolysis of HMF. The Barett-Emmet-Tall (BET) analysis results of the supported Ni catalysts were presented in Table 1.

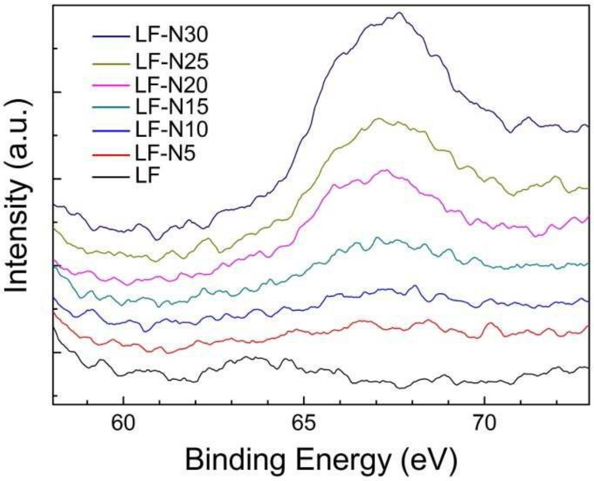

Fig. 3 XPS spectra in the Ni 3p region for perovskite supported Ni catalysts

Table 1 Physico-chemical properties of catalysts

Catalyst	Ni / wt%	D_{MP}[a] / nm	Sureface Area[b] / m^2/g	Pore Volume[c] / cm^3/g	Pore Size[d] / nm
LF-N5	5	15.6	2.54	0.043	40.2
LF-N10	10	16.4	5.55	0.054	61.7
LF-N15	15	18.4	4.67	0.051	53.8
LF-N20	20	21.0	3.35	0.039	53.9
LF-N25	25	24.7	5.88	0.045	51.1
LF-N30	30	26.4	3.76	0.025	37.2
F-N20	20	26.6	12.09	0.085	22.2
L-N20	20	31.8	1.74	0.009	27.2
LF	0	-	4.88	0.045	42.4

a. Crystal size of the metallic Ni phase, calculated from XRD results with Scherrer formula; b. BET Surface Area; c. BJH desorption cumulative volume of pores between 17.0 Å and 3000.0 Å diameter; d. BJH desorption average pore diameter (4V/A).

3.2 Selective hydrogenolysis of HMF

Selective hydrogenolysis of HMF over different catalysts was performed and the products were analyzed by GC-MS and GC. It could be found that 69.3% DMF could be obtained (Table 2, entry 1) when the Ni content in the catalyst was only 5% (catalyst marked as LF-N5), and the by-products were primarily

Table 2 Catalytic performance of various catalysts for the selective hydrogenolysis of HMF[a]

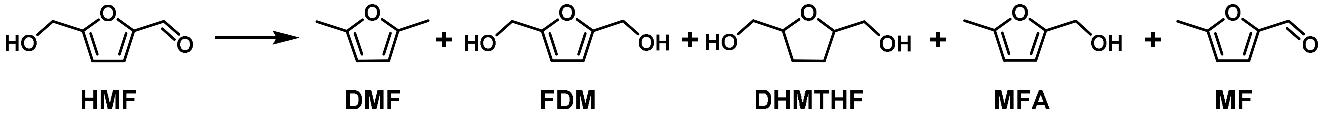

Entry	Catalyst	Conv. / %	Yield / %					
			DMF	FDM	DHMTHF	MFA	MF	Others
1	LF-N5	>99	69.3	0	0	28.7	1.9	0.1
2	LF-N10	>99	74.2	0	0	21.8	1.8	2.2
3	LF-N15	>99	85.9	0	0	10.6	0.9	2.6
4	LF-N20	>99	98.3	0	0	0.7	0.1	0.9
5	LF-N25	>99	86.0	0	7.6	5.6	0	0.8
6	LF-N30	>99	78.1	0	18.1	2.2	0.1	1.5
7	F-N20	>99	67.4	0	1.0	27.8	0.7	3.1
8	L-N20	>99	0	0.1	42.1	0	0.5	57.3
9	LF	96.6	15.3	36.5	0	38.5	2.9	3.4

a. Reaction conditions: 1.0 mmol of HMF, 1.0 mmol of n-tetradecane, 100 mg of the catalyst, 12 ml of ethanol, $P(H_2)$= 5.0 MPa, T= 230 ºC, t= 6.0 h; DMF : 2,5-dimethylfuran; FDM : 2,5-furandimethanol; DHMTHF : 2,5-dihydroxymethyltetrahydrofuran; MFA :5-methylfurfuryl alcohol; MF : 5-methylfurfural.

5-methylfurfuryl alcohol (MFA) and 5-methylfurfural (MF) which could be converted into DMF by further hydrogenolysis. With increasing the Ni content to 10%, the yield of DMF increased slightly to 74.2%, and there was still 21.8% MFA kept unconverted (Table 2, entry 2). The yield of DMF reached to 85.9% when the Ni content was 15%, and only 10.6% MFA and 0.9% MF were remained (Table 2, entry 3). In order to further improve the product yields, we synthesized catalysts with higher Ni content. Nearly quantitative DMF (Table 2, entry 4) was obtained using the LF-N20 as catalyst, which means that the higher Ni contents afford for more active metal sites. However, further increased the Ni contents in the catalysts resulted in over-hydrogenation of HMF. When LF-N25 was used for the hydrogenolysis of HMF, 2,5-dihydroxymethyltetrahydrofuran (DHMTHF) was formed with a yield of 7.6%, and the yield of DMF decreased to 86.0% with 5.6% MFA remained unconverted (Table 2, entry 5). The yield of DHMTHF reached to 18.1% when LF-N30 was used for the hydrogenation of HMF, which indicated more active Ni sites resulted in the over-hydrogenaion (Table 2, entry 6). For comparison, the reaction using iron oxides supported Ni and lanthanum oxides supported Ni (labeled as F-N20 and L-N20, respectively) as catalysts were also investigated, resulted in the yields 67.4% and 0% of DMF, which proved that only the perovskite supported Ni particles was responsible for the better yields. In the case of F-N20, 27.8% MFA and 0.7% MF were the main by-products, which meant the LFN-20 was more efficient for the hydrogenolysis of C-O bonds of MFA. And $LaFeO_3$ (marked as LF) was also investigated for the hydrogenolysis of HMF, DMF yield of 12.2% was obtained suggestting low activity. And 36.5% 2,5-furandimethanol (FDM), 38.5% MFA and 2.9% MF were obtained, which indicated that active Ni particles was necessary for the formation of DMF.

3.3 Effect of reaction temperature

Temperature is one of the important factors for the conversion of HMF to DMF, so the effect of different temperature on the hydrogenolysis of HMF was investigated. It could be confirmed from Figure 4 that the activity was quite low at lower temperature such as 200 °C, although the conversion of HMF reached to 98.6%, DMF yield was only 8.7% at this condition, and the main products were MFA and FDM with yields of 61.9% and 18.1%, respectively. MFA and FDM could be converted into DMF through the cleavage of C-O bonds, this result indicted that hydrogenolysis of HMF was incomplete. Continue to increase the temperature to 210 °C, the yield of DMF rose to 45.8%, showed that higher temperature was necessary for the better activity. And the yields of the main by-products MFA and FDM decreased to

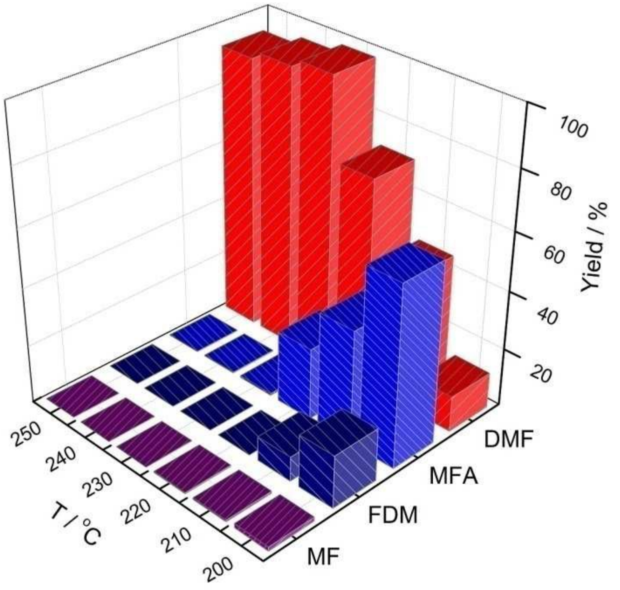

Fig. 4 Effect of different temperature on the conversion of HMF to DMF, Reaction conditions: 1.0 mmol of HMF, 1.0 mmol of n-tetradecane, 100 mg of the LF-N20, 12 ml of ethanol, $P(H_2)$= 5.0 MPa, t= 6.0 h; DMF : 2,5-dimethylfuran; FDM : 2,5-furandimethanol; MFA :5-methylfurfuryl alcohol; MF : 5-methylfurfural.

38.9% and 8.4%, respectively, which indicated that MFA and FDM might be the intermediates in this reation. In order to further improve the yield of DMF, we increased the reaction temperature to 220 ^{o}C, and 71.3% of DMF was obtained, however, FDM was completely converted and the yield of MFA further decreased to 24.7%. The hydrogenolysis reaction reached a maximum yield of 98.3% when the temperature reached to 230 ^{o}C, and the yield of MFA was only 0.7% at this point. Further increasing the reaction temperature to 240 ^{o}C resulted in a slight decrease of the DMF yield which might be attributed to the hydrogenation of DMF to afford 2,5-dimethyltetrahydrofuran (DMTHF), suggesting that side reactions occurred at higher temperature. The investigation on the reaction temperature indicated that temperature had an important impact on the products distribution and a proper temperature was necessary to afford the highest yield of DMF.

3.4 Effect of hydrogen pressure

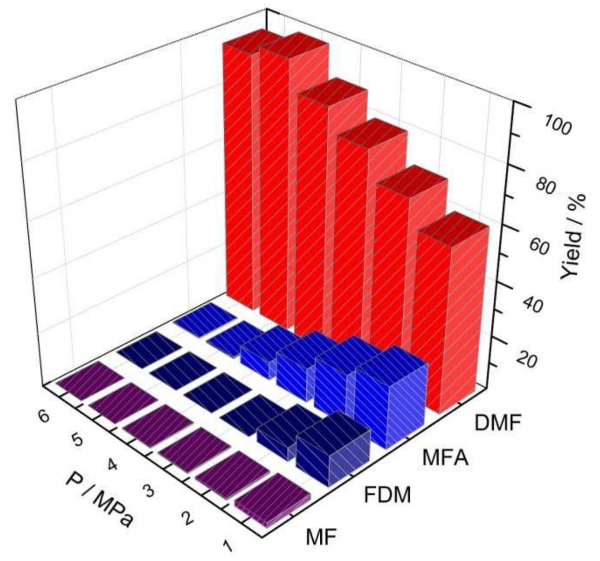

Fig. 5 Effect of H_2 pressure on the hydrogenolysis of HMF to afford DMF, Reaction conditions: 1.0 mmol of HMF, 1.0 mmol of n-tetradecane, 100 mg of the LF-N20, 12 ml of ethanol, T= 230 ^{o}C, t= 6.0 h; DMF : 2,5-dimethylfuran; FDM : 2,5-furandimethanol; MFA :5-methylfurfuryl alcohol; MF : 5-methylfurfural.

The effect of hydrogen pressure on the hydrogenolysis of HMF was investigated to better understand the reaction process. It could be informed from Fig. 5 that the hydrogenolysis of HMF could proceed even under relatively low hydrogen pressure. When the reaction was carried out under a H_2 pressure of 1MPa, the conversion of HMF reached to 97.9%, and the yield of DMF was 60.0%, the by-products were MFA (23.1%), FDM (11.6%) and MF (2.1%), which were not completely hydrogenolysed. When the H_2 pressure increased to 2 MPa, the conversion of HMF was 98.9%, the yield of DMF slightly increased to 69.6%, however, the yields of MFA and FDM decreased to 18.7% and 5.1%, respectively, which implied that high pressure favored the hydrogenolysis of reaction intermediates. When the H_2 pressure was above 2 MPa, the conversions of HMF were >99%. Further increasing the H_2 pressure to 3 MPa led to an improvement of DMF yield (79.7%), however, 12.6% of MFA still remained unconverted. To further improve the yield of DMF, reaction under higher H_2 pressure was investigated, and 87.9% of DMF could be obtained under the pressure of 4 MPa. The yield of DMF reached to nearly equivalent (98.3%) under a H_2 pressure of 5 MPa. However, higher reaction pressure (*e.g.* 6 MPa) did not result in the higher yield of DMF, and 94.6% of DMF was collected, which might be due to the hydrogenation of DMF. The survey on the H_2 pressure revealed that a relatively high H_2 pressure (*e.g.* 5 MPa) was essential to afford DMF, however, too high pressure was not always desired.

3.5 Recyclability of the catalyst

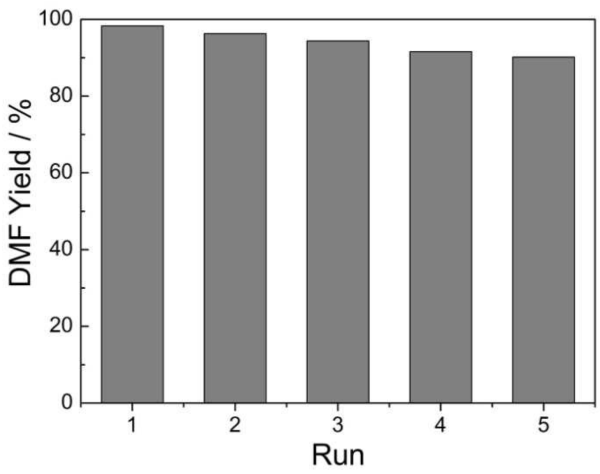

Fig. 6 The recyclability of perovskite supported Ni catalyst. Reaction conditions: 1.0 mmol of HMF, 1.0 mmol of n-tetradecane, 100 mg of the LF-N20, 12 ml of ethanol, $P(H_2)$= 5.0 MPa, T= 230 ^{o}C, t= 6.0 h.

The stability of the catalyst is great importance for the commercial application of the heterogeneous catalysts. To test the stability of the perovskite supported Ni catalyst, the LF-N20 catalyst was collected by centrifugation after the reaction and washed with ethanol for at least five times. Then the catalyst was directly used for the next run. It could be informed from Fig. 5 that the catalyst maintained good activity for the hydrogenolysis of HMF after used for five times. The yield of DMF after the fifth run was still 90.2%, and a possible explanation for the decrease of the DMF yield was the mass loss of the catalyst during the washing process and the formation of by-products on the metal sites of the catalyst, which is in accordance with the previous reports[27].

3.6 Mechanism

The main detected by-products for the hydrogenolysis of HMF were FDM, MF and MFA. In order to establish the reaction sequence, the effect of reaction time on the products distribution for the hydrogenolysis of HMF was investigated. As showed in Fig. 7, at the initial time of the reaction (*e.g.* 0.5 h), HMF was almost completely converted (96.1%). However, the yield of DMF was just 8.3%, the main products were FDM (30.3%) and

MFA (51.6%), it should be noticed that MF was detected with a yield of 2.4% which meant that HMF was transformed into MF directly or indirectly during the hydrogenolysis process. Prolonging the reaction time to 1.0 h resulted in the nearly completely conversion of HMF, and the yield of DMF increased to 31.3%. The yield of MFA reached a maximum (59.4%) during the entire duration of the reaction, whereas FDM yield decreased to 6.3%. Since FDM could be converted into MFA and DMF through selectively cleavage of the C-O bond, therefore the conversion of FDM to MFA and the hydrogenolysis of MFA to DMF were the dominated processes during this period. The DMF yield increased to 53.4% when the reaction time was 2.0 h, meanwhile MFA yield and FDM significantly decreased to 41.8% and 2.2%, respectively. When the reaction time was extended to 4.0 h, 81.5% of DMF was obtained, however, the yield of MFA decreased to 14.9%, which suggested that MFA was an important precursor to be converted into DMF. The yield of DMF increased to 98.3% at a reaction time of 6.0 h, and the yield of the main by-product MFA was only 0.7%. The yield of DMF slightly decreased to 97.3% after further prolonging the reaction time to 10.0 h, which indicated that DMF could existed stably under this kind of reaction conditions.

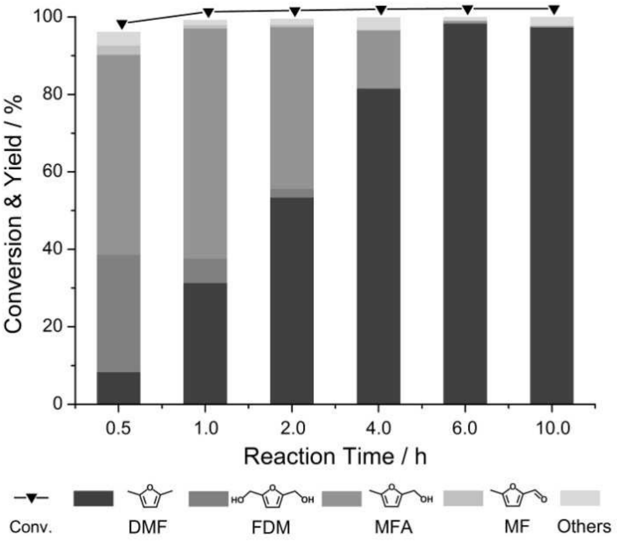

Fig. 7 Effect of time on the conversion of HMF to DMF, Reaction conditions: 1.0 mmol of HMF, 1.0 mmol of n-tetradecane, 100 mg of the LF-N20, 12 ml of ethanol, $P(H_2)$= 5.0 MPa, T= 230 °C; DMF : 2,5-dimethylfuran; FDM : 2,5-furandimethanol; MFA :5-methylfurfuryl alcohol; MF : 5-methylfurfural.

To further investigate the reaction mechanism, the reaction intermediates FDM, MFA, and MF were hydrogenolysed. Reactions using these substrates were carried out under the same reaction conditions to verify that these intermediates could be converted into DMF. As shown in Table 3, FDM, which was obtained through the hydrogenation of C=O bond, could be converted into DMF with a yield of 95.6%. HMF could be transformed into MF through the cleavage of C-O and subsequently hydrogenation of C=O to get MFA, both MF and MFA were hydrogenolysed and high yields of 96.5% and 99.6% were obtained, respectively. DMF was also reacted under the same conditions and the recovery ration was 98.4%. Based on the above results, a possible reaction pathway was proposed, which was similar to the previous reports[27] (Fig. 8). HMF was converted into FDM and MF through two distinctive ways: hydrogenation of C=O bond and hydrogenolysis of C-O bond. Both of FDM and MF were transformed into the main reaction intermediate MFA through the hydrogenolysis of C-O bond and hydrogenation of C=O bond, respectively. And DMF was obtained through hydrogenolysis of C-O bond of MFA.

Table 3 Hydrogenolysis of the reaction intermediates for the mechanism investigation[a]

Entry	Substrate	Conv. / %	DMF yield / %
1	FDM	>99	95.6
2	MF	>99	96.5
3	MFA	>99	99.6
4	DMF	>99	98.4

Reaction conditions: 1.0 mmol of substrate, 1.0 mmol of n-tetradecane, 100 mg of the LFN-20, 12 ml of ethanol, $P(H_2)$= 5.0 MPa, T= 230 °C, t=6.0h.

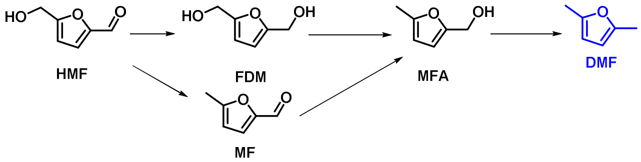

Fig. 8 Possible reaction pathway for the hydrogenolysis of HMF

4 Conclusions

In conclusion, the hydrgenolysis of biomass-derived HMF into DMF has been performed over perovskite supported Ni catalyst system. Under optimized conditions, >99% conversion of HMF with a high DMF yield (98.3%) was achieved. The perovskited catalyst system showed a high stability, it kept the activity after recycled for at least 4 times. The kinetic experiments revealed that HMF was converted into MFA through the reaction intermediates FDM and MF. The current research emphasized an efficient perovskite-based catalyst system for transforming biomass-derived platform compounds into bio-fuels.

Acknowledgements

This work was supported by the 973 Program (2012CB215305, 2012CB215306, 2013CB228103), NSFC (21325208, 21172209, 21272050, 21402181, 21572212), CAS (KJCX2-EW-J02), IPDFHCPST (2014FXCX006), CPSF (2014M561835), SRFDP (20123402130008), FRFCU (WK2060190025, WK2060190033) and PCSIRT. Thanks for the support by the Program for Changjiang Scholars and Innovative Research Team in University of the Ministry of Education of China and the Fundamental Research Funds for the Central Universities (WK 2060190040)

Notes and references

[a] *Collaborative Innovation Center of Chemistry for Energy Materials, CAS Key Laboratory of Urban Pollutant Conversion, Anhui Province Key Laboratory of Biomass Clean Energy and Department of Chemistry, University of Science and Technology of China, 230026, Hefei, Anhui, China. E-mail: fuyao@ustc.edu.cn; Fax: +86-551-6360-6689; Tel: +86-551-6360-6640*

† Electronic Supplementary Information (ESI) available: [details of any supplementary information available should be included here]. See DOI: 10.1039/b000000x/

‡ These authors equally contributed to the work.

1 J. C. Serrano-Ruiz and J. A. Dumesic, *Energy Environ. Sci.*, 2011, **4**, 83.

2 (a) G. W. Huber, S. Iborra and A. Corma, *Chem. Rew.*, 20016, **106**, 4044; (b) E. L.Kunkes, D. A.Simonetti, R. M. West, J. C. Serrano-Ruiz, C. A. Gärtner and J. A. Dumesic, *Science*, 2008, **322**, 417; (c) P. Gallezot, *Chem. Soc. Rev.*, 2012, **41**, 1538; (d) K. Barta and P. C. Ford, *Acc. Chem. Res.*, 2014, **47(5)**, 1503; (e) C. Z. Li, X. C. Zhao, A. Q. Wang, G. W. Huber and T. Zhang, *Chem. Rew.*, 2015, **115**, 11559; (f) A. Corma, S. Iborra and A. Velty, *Chem. Rew.*, 2007, **107**, 2411.

3 (a) N. Yan, C. Zhao, P. J. Dyson, C. Wang,L. T. Liu and Y. Kou, *ChemSusChem*, 2008, **1**, 626; (b) Y. Zhao, Q. Xu, T. Pan, Y. Zuo, Y. Fu and Q. X. Guo. *Appl. Catal., A*, 2013, **467**, 504; (c) M. Y. Chen, Y. B. Huang, H. Pang, X. X. Liu and Y. Fu, *Green Chem.*, 2015, **17**, 1710; (d) Y. B. Huang, L. Yan, M. Y. Chen, Q. X. Guo and Y. Fu, *Green Chem.*, 2015, **17**, 3010; (e) N. Yan, Y. Yuan, R. Dykeman, Y. Kou and P. J. Dyson, *Angew. Chem. Int. Ed.*, 2010, **49**, 5549.

4 (a) M. Besson, P. Gallezot and C. Pinel, *Chem. Rev.*, 2014, **114**, 1827; (b) J. Zakzeski, P. C. A. Bruijnincx, A. L. Jongerius and B. M. Weckhuysen, *Chem. Rev.*, 2010, **110**, 3552.

5 (a) Y. Román-Leshkov, C. J. Barrett, Z. Y. Liu and J. A. Dumesic, *Nature*, 2007, **447**, 982; (b) J. B. Binder and R. T. Raines, *J. Am. Chem. Soc.*, 2009, **131**, 1979.

6 (a) J. J. Bozell and G. R. Petersen, *Green Chem.*, 2010, **12**, 539; (b) R.J. van Putten, J. C. van der Waal, E. de Jong, C. B. Rasrendra, H. J. Heers and J. G. de Vries, *Chem. Rev.*, 2013, **113**, 1499; (c) L. L. Yu, L. He, J. Chen, J. W. Zheng, L. M. Ye, H. Q. Lin and Y. Z. Yuan, *Chemcatchem*, 2015, **11**, 1701.

7 (a) N. Yoshida, N. Kasuya, N. Haga and K. Fukuda, *Polym. J.*, 2008, **40**, 1164; (b) M. Tamura, K. Tokonami, Y. Nakagawa and K. Tomishige, *Chem. Commun.*, 2013, **49**, 7034; (c) S. Subbiah, S. P. Simeonov, J. M. S. S. Esperança, L. P. N. Rebelo and C. A. M. Afonso, *Green Chem.*, 2013, **15**, 2849; (d) A. J. Kumalaputri, G. Bottari, P. M. Erne, H. J. Heers and K. Barta, *Chemsuschem*, 2014, **7**, 2266; (e) M. Balakrishnan, E. R. Sacia and A. T. Bell, *Green Chem.*, 2012, **14**, 1626; (f) R. Q. Fang, H. L. Liu, R. Luque and Y. W. Li, *Green Chem.*, 2015, **17**, 4183; (g) C. Aellig, F. Jenny, D. Scholz, P. Wolf, I. Giovinazzo, F. Kollhoff and I. Hermans, *Catal. Sci. Technol.*, 2014, **4**, 2326; (h) S. Dutta, S. De and B. Saha, *Chempluschem*, 2012, **77**, 259.

8 (a) H. A. Rass, N. Essayem and M. Besson, *Green Chem.*, 2013, **15**, 2240; (b) N. K. Gupta, S. Nishimura, A. Takaqaki and K. Ebitani, *Green Chem.*, 2011, **13**, 824; (c) J. Y. Cai, H. Ma, J. J. Zhang, Q. Song, Z. T. Du, Y. Z. Huang and J. Xu, *Chem. – Eur. J.*, 2013, **19**, 14215; (d) H. A. Rass, N. Essayem and M. Besson, *Chemsuschem*, 2015, **8**, 1206; (e) C. M. Zhou, W. P. Deng, X. Y. Wan, Q. H. Zhang, Y. H. Yang and Y. Wang, *Chemcatchem*, 2015, **7**, 2853; (f) X. Y. Wan, C. M. Zhou, J. S. Chen, W. P. Deng, Q. H. Zhang, Y. H. Yang and Y. Wang, *ACS Catal.*, 2014, **4**, 2175; (g) W. P. Dijkman, D. E. Groothuis and M. W. Fraaije, *Angew. Chem. Int. Ed.*, 2014, **53**, 6515; (h) Z. H. Zhang, J. D. Zheng, B. Liu, K. Lv and K. J. Deng, *Green Chem.*, 2015, **17**, 1308; (i) N. Mei, B. Liu, J. D. Zheng, K. Lv, D. G. Tang and Z. H. Zhang, *Catal. Sci. Technol.*, 2015, **5**, 3194.

9 X. L. Tong, Y. Ma and Y. D. Li, *Appl. Catal., A*, 2010, **385**, 1.

10 (a) K. K. Höinghaus, P. Oßwald, T. A. Cool, T. Kasper, N. Hansen, F. Qi, C. K. Westbrook, and P. R. Westmoreland, *Angew. Chem. Int. Ed.*, 2010, **49**, 3572; (b) A. K. Agarwal, *Prog. Energy Combust. Sci.*, 2007, **33**, 233; (c) A. Demirbas, *Prog. Energy Combust. Sci.*, 2007, **33**, 1; (d) O. R. Inderwildi and D. A. King, *Energy Environ. Sci.*, 2009, **2**, 343.

11 Y. Qian, L. F. Zhu, Y. Wang and X. C. Lu, *Renew. Suatain. Energy Rev.*, 2015, **41**, 633.

12 (a) B. Saha and M. M. A. Omar, *Chemsuschem*, 2015, **8**, 1133; (b) L. Hu, Y. Sun and L. Lin, *Prog. Chem.*, 2011, **23**, 2079; (c) A. S. Nagpure, N. Lucas and S. V. Chilukuri, *ACS Sustainable Chem. Eng.*, 2015, **3**, 2909; (d) B. Saha, M. H. Fan and J. J. Wang, *Sustainable Catalytic Processes*, 2015, Elsevier.

13 (a) M. Chidambaram and A. T. Bell, *Green Chem.*, 2010, **12**, 1253; (b) T. Thananatthanachon and T. B. Rauchfuss, *Angew. Chem. Int. Ed.*, 2010, **49**, 6616; (c) M. Chatterjee, T. Ishizaka and H. Kawanami, *Green Chem.*, 2014, **16**, 1543; (d) F. Liu, M. Audemar, K. D. O. Vigier, J. M. Clacens, F. D. Campo and F. Jérôme, *Chemsuschem*, 2014, **7**, 2089; (e) F. Liu, M. Audemar, K. D. O. Vigier, J. M. Clacens, F. D. Campo and F. Jérôme, *Green Chem.*, 2014, **16**, 4110; (f) J. Mitra, X. Y. Zhou and T. Rauchfuss, *Green Chem.*, 2015, **17**, 307.

14 (a) S. De, S. Dutta and B. Saha, *Chemsuschem*, 2012, **5**, 1826; (b) J. Jae, W. Q. Zheng, R. F. Lobo and D. G. Vlachos, *Chemsuschem*, 2013, **6**, 1158; (c) L. Hu, X. Tang, J. Xu, Z. Wu, L. Lin and S. J. Liu, *Ind. Eng. Chem. Res.*, 2014, **53**, 3056; (d) J. Jae, W. Q. Zheng, A. M. Karim, W. Guo, R. F. Lobo and D. G. Vlachos, *Chemcatchem*, 2014, **6**, 848; (e) C. Z. Li, H. L. Cai, B. Zhang, W. Z. Li, G. X. Pei, T. Dai, A. Q. Wang and T. Zhang, *Chin. J. Catal.*, 2015, **36**, 1638.

15 J. M. R. Gallo, D. M. Alonso, M. A. Mellmer and J. A. Dumesic, *Green Chem.*, 2013, **15**, 85.

16 N. Lucas, N. R. Kanna, A. S. Nagpure, G. Kokate and S. Chilukuri, *J. Chem. Sci.*, 2014, **126**, 403.

17 S. Nishimura, N. Ikeda and K. Ebitani, *Catal. Today*, 2014, **232**, 89.

18 B. Saha, C. M. Bohn and M. M. A. Omar, *Chemsuschem*, 2014, **7**, 3095.

19 D. Scholz, C. Aellig and I. Hermans, *Chemsuschem*, 2014, **7**, 268.

20 G. H. Wang, J. Hilgert, F. H. Richter, F. Wang, H. J. Bongard, B. Spliethoff, C. Weidenthaler and F. Schüth, *Nat. Mater.*, 2014, **13**, 293.

21 (a) J. J. Wang, X. H. Liu, B. C. Hu, G. Z. Lu and Y. Q. Wang, *RSC Adv.*, 2014, **4**, 31101; (b) Y. H. Zu, P. P. Yang, J. J. Wang, X. H. Liu, J. W. Ren, G. Z. Lu and Y. Q. Wang, *Appl. Catal., B*, 2014, **146**, 244.

22 G. Y. Jeong, A. K. Singh, S. Sharma, K. W. Gyak, R. A. Maurya and D. P. Kim, *NPG Asia Mater.*, 2015, **7**, 1.

23 J. Luo, L. A. Ramírez and R. J. Gorte, *AIChE J.*, 2015, **61**, 590.

24 A. S. Nagpure, A. K. Venugopal, N. Lucas, M. Manikandan, R. Thirumalaiswamy and S. Chilukuri, *Catal. Sci. Technol.*, 2015, **5**, 1463.

25 P. P. Upare, D. W. Hwang, Y. K. Hwang, U. H. Lee, D. Y. Hong and J. S. Chang, *Green Chem.*, 2015, **17**, 3310.

26 X. J. Cui, X. C. Dai, Y. Q. Deng and F. Shi, *Chem. – Eur. J.*, 2013, 19, 3665.

27 X. Kong, Y. F. Zhu, H. Y. Zheng, F. Dong, Y. L. Zhu and Y. W. Li, *RSC Adv.*, 2014, **4**, 60467.

28 X. Kong, R. X. Zheng, Y. F. Zhu, G. Q. Ding, Y. L. Zhu and Y. W. Li, *Green Chem.*, 2015, **17**, 2504.

29 X. Kong, Y. F. Zhu, H. Y. Zheng, X. Q. Li, Y. L. Zhu and Y. W. Li, *ACS Catal.*, 2015, **5**, 5914.

30 P. P. Yang, Q. Q. Cui, Y. H. Zu, X. H. Liu, G. Z. Lu and Y. Q. Wang, *Catal. Commun.*, 2015, **66**, 55.

31 L. L. Yu, L. He, J. Chen, J. W. Zheng, L. M. Ye, H. Q. Lin and Y. Z. Yuan, *Chemcatchem*, 2015, **7**, 1701.

32 (a) T. S. Hansen, K. Barta, P. T. Anastas, P. C. Ford and A. Riisager, *Green Chem.*, 2012, **14**, 2457; (b) A. J. Kumalaputri, G. Bottari, P. M. Erne, H. J. Heeres and K. Barta, *Chemsuschem*, 2014, **7**, 2266.

33 G. Bottari, A. J. Kumalaputri, K. K. Krawczyk, B. L. Feringa, H. J. Heeres and K. Barta, *Chemsuschem*, 2015, **8**, 1323.

34 Y. F. Zhu, X. Kong, H. Y. Zheng, G. Q. Ding, Y. L. Zhu and Y. W. Li, *Catal. Sci. Technol.*, 2015, **5**, 4208.

35 (a) J. M. Simmie and J. Würmel, *Chemsuschem*, 2013, **6**, 36; (b) X. L. Tong, Y, Ma and Y. D. Li, *Appl. Catal., A*, 2010, **385**, 1; (c) Y. Nakagawa, M. Tamura and K. Tomishige, *ACS Catal.*, 2013, **3**, 2655; (d) L. Hu, L. Lin and S. J. Liu, Ind. Eng. *Chem. Res.*, 2014, **53**, 9969; (e) S. De, B. Saha and R. Luque, *Bioresour. Technol.*, 2015, **178**, 108; (f) M. J. Climent, A. Corma and S. Iborra, *Green Chem.*, 2014, **16**, 516; (g) H. Li, P. S. Bhadury, A. Riisager and S. Yang, *Catal. Sci. Technol.*, 2014, **4**, 4138.

36 Y. B. Huang, M. Y. Chen, L. Yan, Q. X. Guo and Y. Fu, *Chemsuschem*, 2014, **7**, 1068.

37 (a) S. Royer, D. Duprez, F. Can, X. Courtois, C. B. Dupeyrat, S. Laassiri and H. Alamdari, *Chem. Rev.*, 2014, **114**, 10292; (b) R. F. Savinell, *Nat. Chem.*, 2011, **3**, 501; (c) J. J. Zhu, H. L. Li, L. Y. Zhong, P. Xiao, X. L. Xu, X. G. Yang, Z. Zhao and J. L. Li, *ACS Catal.*, 2014, **4**, 2917; (d) J. J. Xu, D. Xu, Z. L. Wang, H. G. Wang, L. L. Zhang and X. B. Zhang, *Angew. Chem. Int. Ed.*, 2013, **52**, 3887; (e) T. Oshima, D. L. Lu, O. Ishitani and K. Maeda, *Angew. Chem. Int. Ed.*, 2015, **54**, 2698; (f) B. Siritanaratkul, K. Maeda, T. Hisatomi and K. Domen, *Chemsuschem*, 2011, **4**, 74; (g) O. A. Marina, N. L. Canfield and J. W. Stevenson, *Solid State Ionics*, 2002, **149**, 21; (h) H. Kato, H. Kobayashi and A. Kudo, *J. Phys. Chem. B*, 2002, **106**, 12441; (i) R. J. H. Voorhoeve, J. P. Remeika and L. E. Trimble, *Ann. NY. Acad. Sci.*, 2006, **272**, 3; (j) W. F. Yao, X. H. Xu, H. Wang, J. T. Zhou, X. N. Yang, Y. Zhang, S. X. Shang and B. B. Huang, *Appl. Catal., B*, 2004, **52**, 109; (k) T. Poux, F. S. Napolskiy, T. Dintzer, G. Kéranguéven, S. Y. Isomin, G. A. Tsirlina, E. V. Antipov and E. R. Savinova, *Catal. Today*, 2012, **189**, 83.

38 (a) J. Suntivich, H. A. Gasteiger, N. Yabuuchi, H. Nakanishi, J. B. Goodenough and Y. S. Horn, *Nature Chem.*, 2011, **3**, 546; (b) J. Kim, S. Choi, A. Jun, H. Y. Jeong, J. Shin and G. Kim, *Chemsuschem*, 2014, **7**, 1669; (c) Y. L. Lee, J. Kleis, J. Rossmeisl and D. Morgan, *Phys. Rev. B*, 2009, **80**, 224101; (d) Y. F. Sun, Y. Q. Zhang, B. Hua, Y. Behnamian, J. Li, S. H. Cui, J. H. Li and J. L. Luo, *J. Power Sources*, 2016, **301**, 237.

39 (a) J. Burschka, N. Pellet, S. J. Moon, R. H. Baker, P. Gao, M. K. Nazeeruddin and M. Grätzel, *Nature*, 2013, **499**, 316; (b) M. M. Lee, J. Teuscher, T. Miyasaka, T. N. Murakami and H. J. Snaith, *Science*, 2012, **338**, 643; (c) M. Z. Liu, M. B. Johnson and H. J. Snaith, *Nature*, 2013, **501**, 395; (d) G. C. Xing, N. Mathews, S. Y. Sun, S. S. Lim, Y. M. Lam, M. Grätzel, S. Mhaisalkar and T. C. Sum, *Science*, 2013, **342**, 344; (e) H. P. Zhou, Q. Chen, G. Li, S. Luo, T. B. Song, H. S. Duan, Z. R. Hong, J. B. You, Y. S. Liu, Y. Yang, *Science*, 2014, **345**, 542; (f) N. J. Jeon, J. H. Noh, Y. C. Kim, W. S. Yang, S. Ryu and S. I. Seok, *Nat. Mat.*, 2014, **13**, 897; (g) J. H. Heo, S. H. Im, J. H. Noh, T. N. Mandal, C. S. Lim, J. A. Chang, Y. H. Lee, H. J. Kim, A. Sarkar, M. K. Nazeeruddin, M. Grätzel and S. I. Seok, *Nat. Photon.*, 2013, **7**, 486.

40 (a) Y. Nishihata, J. Mizuki, T. Akao, H. Tanaka, M. Uenishi, M. Kimura, T. Okamoto and N. Hamada, *Nature*, 2002, **418**, 164; (b) J. Suntivich, K. J. May, H. A. Gasteiger, J. B. Goodenough and Y. S. Horn, *Science*, 2011, **334**, 1383; (c) R. J. H. Voorhoeve, D. W. J. Jr, J. P. Remeika and P. K. Gallagher, *Science*, 1977, **195**, 827; (d) R. J. H. Voorhoeve, J. P. Remeika and D. W. J. Jr, *Science*, 1973, **180**, 62; (e) J. I. Jung, H. Y. Jeong, J. S. Lee, M. G. Kim and J. Cho, *Angew. Chem. Int. Ed.*, 2014, **53**, 4582.

41 D. J. Chen, C. Chen, Z. M. Baiyee, Z. P. Shao and F. Ciucci, *Chem. Rev.*, 2015, **115**, 9869.

42 K. H. Lin, C. B. Wang and S. H. Chien, *Int. J. Hydrogen Energy*, 2013, **38**, 3226.

43 N. Escalona, W. Aranzaez, K. Leiva, N. Martínez and G. Pecchi, *Appl. Catal., A*, 2014, **481**, 1.

44 (a) S. Q. Chen and Y. Liu, *Int. J. Hydrogen Energy*, 2009, **34**, 4735; (b) S. Q. Chen, H. Wang and Y. Liu, *Int. J. Hydrogen Energy*, 2009, **34**, 7995; (c) S. Q. Chen, Y. D. Li, Y. Liu and X. Bai, *Int. J. Hydrogen Energy*, 2011, **36**, 5849.

45 (a) L. J. Zhu, P. J. Guo, X. W. Chu, S. R. Yan, M. H. Qiao, K. N. Fan, X. X. Zhang and B. N. Zong, *Green Chem.*, 2008, **10**, 1323; (b) J. F. Moulder, W. F. Stickle, P. E. Sobol and K. D. Bomben, *Handbook of X-ray Photoelectron Spectroscopy*, J. Chastain, (Ed.), Perkin-Elmer, Eden Prairie, MN, 1992.

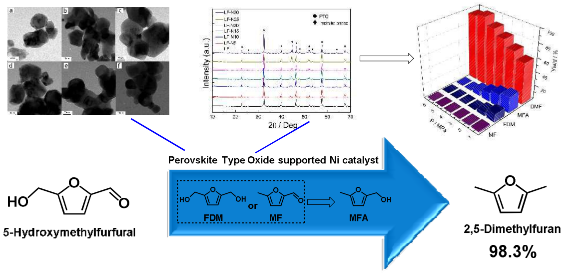

Hydrogenolysis of biomass-derived 5-hydroxymethylfurfural to 2,5-dimethylfuran was performed over perovskite type oxide supported Ni catalysts, 98.3% of 2,5-dimethylfuran was obtained.